INSTITUTE OF PHYSICS PUBLISHING NANOTECHNOLOGY
Nanotechnology **15** (2004) 457–466 PII: S0957-4484(04)69059-3

A novel and rapid method for quantification of magnetic nanoparticle–cell interactions using a desktop susceptometer

Valter Ström[1,5], Kjell Hultenby[2], Cordula Grüttner[3], Joachim Teller[3], Bo Xu[4] and Jan Holgersson[4]

[1] MSE-Tmfy, Royal Institute of Technology, S-100 44 Stockholm, Sweden
[2] Clinical Research Centre, Karolinska Institutet, Huddinge University Hospital AB, S-141 86 Stockholm, Sweden
[3] micromod Partikeltechnologie GmbH, D-18119 Rostock, Germany
[4] Division of Clinical Immunology F-79, Karolinska Institutet, Huddinge University Hospital AB, S-141 86 Stockholm, Sweden

E-mail: valter@kth.se

Received 8 September 2003, in final form 2 December 2003
Published 2 February 2004
Online at stacks.iop.org/Nano/15/457 (DOI: 10.1088/0957-4484/15/5/009)

Abstract
Activated endothelial cells (EC) are attractive prime targets for specific drug delivery using drug-carrying magnetic nanoparticles. In order to accomplish EC targeting, the interaction between magnetic particles and resting as well as activated endothelial cells must be characterized and quantified, because it will influence particle biodistribution, circulation half-time, and targeting efficacy. Here, we have quantified *in vitro* the interaction (adhesion/phagocytosis) between human endothelial cells and magnetite (Fe_3O_4) particles carrying different surface coatings with varying degrees of hydrophilicity and surface charge. Almost no adhesion was observed (about 1% or less) for three out of five particle types carrying plain dextran, carboxyl-substituted poly(ethylene glycol) and silica C18 coatings. In contrast, carboxyl-functionalized dextran and poly(ethylene glycol)-coated particles adhered or were phagocytosed to a considerable degree (58 and 26%, respectively). These clear and accurate results were obtained by measuring the magnetic response, i.e. magnetic susceptibility, from different fractions of the cell cultures as a means of determining the concentration of magnetic particles. Visible light and electron microscopy confirmed the magnetic quantification. To meet the need for a rapid yet sensitive instrument, we have developed a desktop magnetic susceptometer especially adapted for liquid samples or particles in a suspension. Despite its very high sensitivity, it is easy to operate and requires but a few seconds for a measurement. We also describe the construction and operation of this instrument.

1. Introduction

The number of *in vitro* applications for magnetic microparticles and nanoparticles has increased dramatically during recent years. One example is the use of magnetic particles for isolation of specific cells out of a complex mixture of cells. This has facilitated biological characterization of many cell types of low abundance in a tissue or body fluid [1, 2]. Purified cells with specific features can also be obtained for cell-based thera-

[5] Author to whom any correspondence should be addressed.

pies [3]. Magnetic particles have been used in assays in which a disease-causing microbe is enriched from a body fluid prior to its molecular identification, for example by the polymerase chain reaction (PCR) [4]. Other applications of magnetic particles include the purification of biomolecules such as DNA [5] and proteins [6], which is frequently done in microlitre-sized multi-well systems (reviewed in [7]).

In contrast to the numerous novel *in vitro* applications for magnetic particles, new therapeutic or diagnostic *in vivo* uses are scarce. Besides the use of magnetic nanoparticles in magnetic imaging [8, 9], such particles are expected to contribute to the development of improved gene and drug delivery strategies [7, 10]. The goal of such strategies is to accomplish a high local concentration of the curing drug at the diseased target tissue, while the systemic concentration is low. This can dramatically reduce side effects and improve therapeutic efficacy [11, 12]. A magnetic field gradient (from an external or internal magnet) is used to guide the drug-carrying magnetic particles to the desired site of action [11, 12].

To investigate specific cell targeting *in vitro* (prior to *in vivo* experimentation), the interaction between magnetic nanoparticles and the cell type to be targeted, or avoided, *in vivo* must be quantified. There are few options in terms of techniques for such quantification. Because of the small particle size, usually <150 nm, visible light microscopy is not a viable option. Scanning and transmission electron microscopy (SEM, TEM) can easily image the particles, but do not allow an accurate average adhesion to be easily obtained over the full cell sample surface. Also, at least the sample preparation for TEM is cumbersome. Alternatively, the magnetic response, e.g. magnetic susceptibility, of a bulk sample could be used to quantify the amount of magnetic particles bound to a cell layer following its lysis. Here, the measurement detects the contribution from every magnetic entity within the sample, thus constituting a perfect average. Although traditional magnetometry (e.g. superconducting quantum interference device (SQUID) or vibrating sample magnetometry (VSM)) is quite suitable for this purpose, the measurements are mostly very time-consuming. Since biological experiments usually generate many samples a traditional approach appears unsuitable. Therefore, we have developed a very sensitive desktop magnetic susceptometer, which is very easy to operate and requires but a few seconds for a measurement.

It is noteworthy that despite the magnetic properties of nanosized magnetic particles being highly interesting and constituting an active research area on their own, those aspects are only secondary in this work, since we are only using the magnetic susceptibility as a means of determining the magnetic particle concentration.

The measurement of magnetic susceptibility, i.e. change in magnetization as a result of an applied magnetic field, is widespread for many applications. Using an alternating (AC) magnetic field at a particular frequency, it is natural to build a completely electronic device for this purpose [13]. More than 70 years ago, Hartshorn described an electrical apparatus, which may be regarded as the archetype of the magnetic AC susceptometer [14]. It comprises one coil (which may be divided into two sections), which is fed by an alternating current (AC) and thus creates the applied field, and one pair of nominally identical pick-up coils positioned within the first coil. The sample is introduced into one member of the pair of pick-up coils. The pick-up coils sense the flux changes as an output voltage, and are electrically connected in series opposition, thereby yielding zero signal without a sample. The sensitivity of such an arrangement is theoretically set by the geometry of the coils, the electrical conductivity of the wire material in the coils and the temperature at which the instrument operates. For best performance, the coil dimensions must be adjusted to sample size. However, a theoretical calculation and a concomitant practical test will reveal that the usable sensitivity will possibly be many orders of magnitude worse than predicted, because the dimensional stability of the coil assembly must be extreme. The total coil assembly should be stable within approximately one part in ten millions. This is a major problem in AC susceptometry.

Here, we describe the desktop susceptometer and its application to accurately quantify low concentrations of magnetic nanoparticles interacting with EC.

2. Materials and methods

2.1. The desktop susceptometer

Dimensional stability of the coil assembly is of utmost importance. This means that inter- and intra-coil distances must be tightly fixed and that the coil assembly must have a uniform temperature. This is realized by casting the coils (figure 1) in a hard and highly thermally conducting epoxy resin with a not too high coefficient of thermal expansion; Young's modulus is 7.5 GPa, the thermal conductivity 1.4 W K^{-1} m^{-1} and the coefficient of thermal expansion is around 30 ppm K^{-1}.

In practice, the combined output from the pick-up coil pair will always display a signal even without a sample. For best performance, this output must be further *electrically balanced*. By letting the innermost layer of each pick-up coil constitute an individual winding we have a signal that is suitable for the required compensation. These signals are proportional to the pick-up coil signals regardless of small changes in dimension or temperature. The extra resistance in series with the two pick-up coils contributes negligibly to the noise performance. Dimensions and some relevant properties of the coils are given in table 1.

During measurements, the *magnetic interaction* with the environment should be weak. One approach, but an inconvenient one, is to keep the coil assembly in a magnetic shield. Instead, we have arranged the pick-up coils in an anti-parallel geometry. Thus, at distances large compared to the dimensions of the coil assembly, the overall response is a quadrupole, since each pick-up coil is equivalent to a dipole. In principle, this arrangement is not sensitive to *any* ambient magnetic field.

It is imperative to achieve a *filling fraction* as high as possible. A convenient sample holder for both liquids and powder is a 'PCR' tube (this item is specified further down) with slightly less than 6 mm diameter; thus we have chosen a 6 mm bore as the measuring zone. The geometry of the pick-up coils, the electrical conductivity of the wire material (which should be high) and the operating temperature set the theoretical noise limit.

In order to utilize a good noise performance, it is also necessary to obtain a *proper matching* between the noise

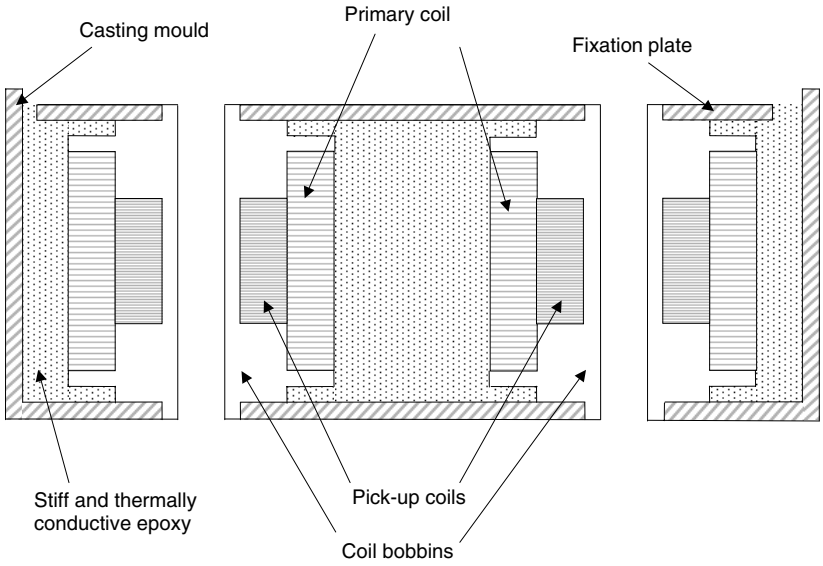

Figure 1. The complete assembly of the cast coils in the casting mould. After casting, the coil assembly becomes a compact block of a stiff and thermally conductive material.

Table 1. Characteristics of the coils.

Coil type	Winding cross section (mm)	Wire diameter (mm)	Number of turns	Resistance (Ω)	Inductance (mH)	Resonance frequency (kHz)
Half-primary	20 × 5.3	0.32	755	9.4	5.2	140
Each pick-up	11 × 3	0.14	1455	56	10.1	120
Each comp. winding	11 × —	0.14	115	6.1	0.08	≫100

resistance of the pick-up coils and the noise resistance of the detecting unit. Selecting the dimension of the wire can in principle do this matching, but in practice this leads to a thin wire susceptible to breaking. Therefore, a preamplifier around the op amp LT1028 (Linear Technology) with particularly low input voltage noise was designed to allow for a convenient wire gauge; figure 2.

The *nominal sensitivity* for a sample small compared to the coil dimensions is straightforward to calculate. It is a matter of calculating the current to field relation in the centre of the (half-)primary and multiplying this with the equivalent current to field relation for the pick-up coil. The second step in this calculation is due to the reciprocity theorem. These field calculations need to consider the finite thickness and size of the windings, i.e. the trivial formula $H = nI$ is modified to $H = nIG$, where H, n, I are the magnetic field (A m^{-1}), number of turns per unit length (m^{-1}) and current in the coil (A) and G is a geometric factor less than one but of order unity depending on the exact geometry of the winding.

With actual numbers ($I = 22.5$ mA$_{\rm rms}$ at $f = 2.00$ kHz, and with a preamplifier with a gain of 21) we get: $\chi V = 5.0 \times 10^{-8} u_{\rm rms}$ (m^3), where $u_{\rm rms}$ is the voltage detected by the lock-in amplifier (SR830, Stanford Research Systems) (V).

From a *calibration* with a purely paramagnetic salt (16.39 mg of $MnSO_4{\cdot}H_2O$ measured into a SQUID magnetometer) we deduce: $\chi V = 5.4 \times 10^{-8} u_{\rm rms}$ (SI). We explain this rather small discrepancy, about 7%, as due to the mutual interaction between the two coil units being neglected in the theoretical calculation.

Although the actual sample geometry is rather different in the measurements of the suspensions where we fill the sample tubes with 60 μl, we find that the sensitivity is essentially unaffected. We can conclude this by measuring the response from a sample tube filled with $MnSO_4{\cdot}H_2O$ occupying the same space as the 60 μl suspension. By weighing this amount it is clear that the response is proportional to the sample weight. Thus, the sensitivity is unaffected and the relation $\chi V = 5.4 \times 10^{-8} u_{\rm rms}$ still holds.

The theoretical detection limit, e.g. defined as the thermal noise from the two pick-up coils, is at room temperature about 0.7 nV$_{\rm rms}$ in a bandwidth of 1 Hz. In real life we use a substantially wider bandwidth of about 100 Hz. Still, the limiting factor is rather thermal drift during the time of measurement. This is roughly 5–20 times worse than the theoretical limit. Thus, there is still room for substantial improvement.

Operation is straightforward. In our set-up we employ a digital two-channel lock-in amplifier (SR830), which incorporates a sufficiently strong signal generator so further amplification of the excitation current is unnecessary. The 5 V$_{\rm rms}$ output is directly connected to the primary with a current sensing resistor in series. The phase is adjusted with a lossless sample (paramagnetic salt) so the in-phase and the out-of-phase voltages are displayed in each channel. With the particles used in this work and with the sensitivity requirements, we have chosen a measuring frequency of 2 kHz.

After having verified proper settings of phase, frequency and amplitude of excitation, the operation is as follows:

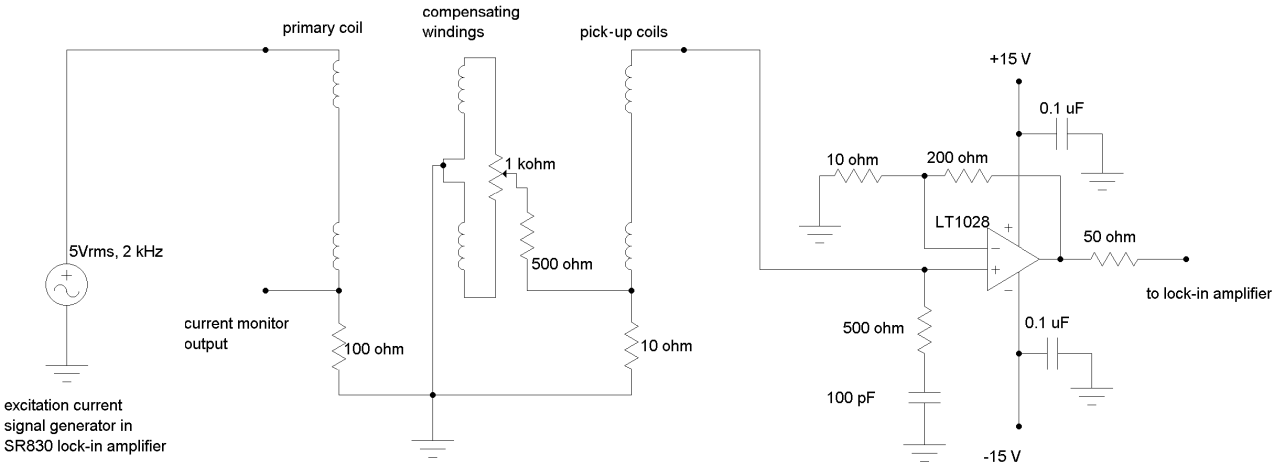

Figure 2. An electrical schematic diagram of the coil assembly and preamplifier. The excitation current is taken directly from the built-in signal generator in the SR830 lock-in amplifier.

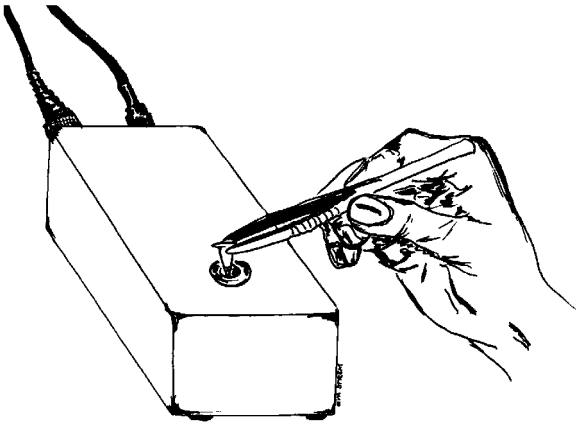

Figure 3. The desktop susceptometer footprint is only 8×15 cm^2. The picture shows a typical sample insertion situation in which the sample is handled with tweezers.

(i) On pressing the 'auto-offset' button, the value displayed in the corresponding channel is zeroed.

(ii) Immediately after zeroing the sample tube is slipped into the bore of one of the primary pick-up units and the value shown is noted. The sample tubes should be handled with non-magnetic tweezers, since a human hand too close to the sensing coil would give rise to an additional signal masking the sample contribution (figure 3).

(iii) The sample tube is retrieved and a check is made to verify that the displayed value returns to zero.

(iv) The above sequence is carried out for both channels.

To further illustrate this procedure we show in figure 4 the two responses versus time where we have made measurements in sequence on the paramagnetic calibration sample, a piece of a 0.6 mm Cu wire and a typical sample with a suspension of magnetic particles. The Cu wire should at these rather low frequencies only have an out-of-phase response, the paramagnetic calibration only an in-phase response and the particle suspension, both.

2.2. Endothelial cell culture

Primary HAECs (Cascade Biologics, Portland, OR) were cultured in gelatin (0.2%)-coated plastic flasks in Medium 200 (Cascade Biologics) supplemented with the LSGS Kit (Cascade Biologics). The cells were cultured at 37 °C in a 5% CO_2 atmosphere, and the culture medium was changed every 48–72 h.

2.3. Magnetic nanoparticles

The particles used (table 2) were produced by micromod Partikeltechnologie GmbH (Rostock, Germany) and were suspended in a physiological saline solution at a concentration of 10 mg of particles/ml. Plain nanomag®-D particles were prepared by processing magnetite aggregates (d = 200–250 nm) with dextran T40 (Roth GmbH, Germany) in a microfluidizer device (Microfluidizer Int. Corp., USA). These plain composite particles possessing a hydrodynamic diameter of 148 nm contain deaggregated magnetite with domain sizes of 15–20 nm embedded in a dextran matrix.

The COOH modified particles were obtained by acylation of plain particles with citric acid in the presence of water-soluble carbodiimide, the PEG-COOH modified particles were prepared in a similar manner using 3,6-dioxaoctanedioic acid and the nanomag®-D PEG 300 (D PEG 300) surface was obtained by esterification of D COOH modified particles with polyethylene glycol 300. Nanomag®-silica C18 (silica C18) particles were synthesized by cross-linking dextran strands of plain particles with silica nanostructures (silica fortification [15]). Thus, reaction of glycidyloxypropyl (trimethoxy)silane with plain particles in the presence of octadecyl (trimethoxy)silane leads to intercalation of C18 containing silica in the outer particle matrix. These particle modifications apply only to the particle surface, so they all have the same core structure.

A major hysteresis loop of 50 μl D plain particle suspension (with a concentration corresponding to 100 μg ml^{-1} of iron) measured in our SQUID magnetometer is displayed in figure 5. Despite the material not being strictly (super)paramagnetic, the remanence is quite low. From figure 5

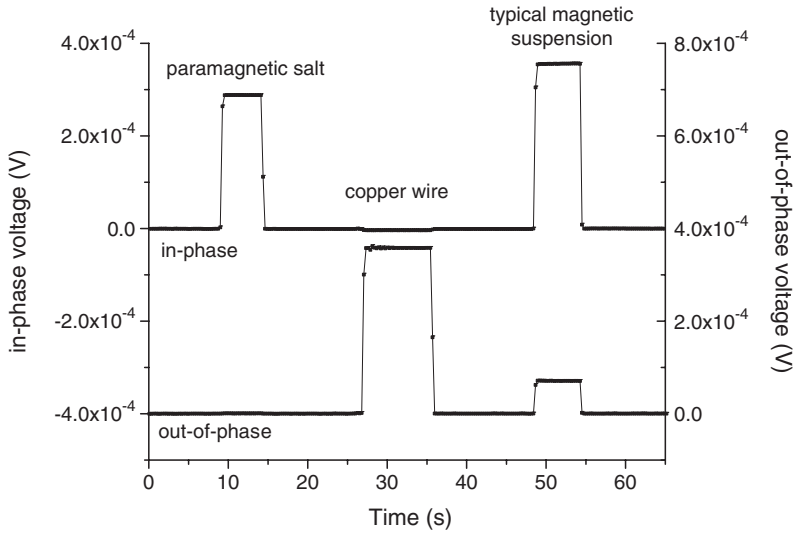

Figure 4. Voltage (susceptibility) responses versus time for a paramagnetic reference sample (16.39 mg of $MnSO_4 \cdot H_2O$), a piece of a 0.6 mm diameter copper wire and a typical sample of a magnetic suspension. The clear discrimination between a paramagnetic in-phase response and a (mostly) dissipative out-of-phase response suggests a proper phase adjustment.

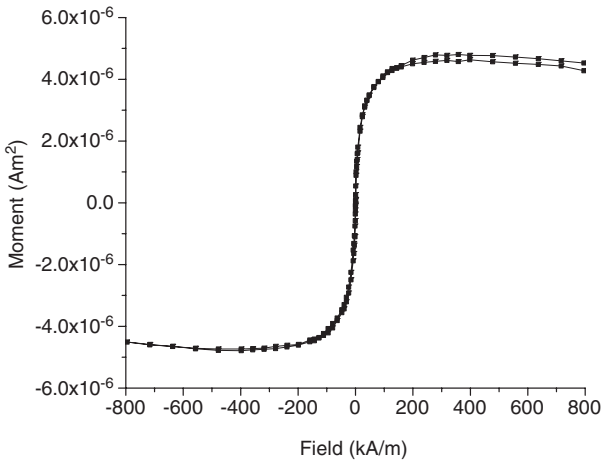

Figure 5. Moment versus field for a 50 μl D plain sample with a concentration corresponding to 100 μg ml^{-1} of iron at 300 K (SQUID measurement).

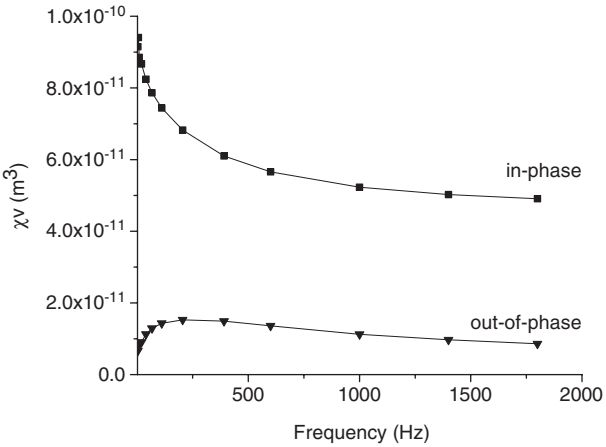

Figure 6. Susceptibility versus frequency for a 50 μl D plain sample with a concentration corresponding to 100 μg ml^{-1} of iron at 300 K and 600 A m^{-1} field strength.

we find that it is below about 1% of the saturation magnetization. The negative slope apparent at higher field strengths is due to the diamagnetic fluid (water) and sample holder.

To ensure that our measuring frequency of 2 kHz does not fall in a frequency interval where the susceptibility happens to be strongly frequency dependant, we have also measured this dependence from a rather low frequency, i.e. 4 Hz, to 2 kHz (i.e. 1.8 kHz); figure 6. Apart from a fairly steep fall going to the very lowest frequencies, there is but a very slight frequency dependence.

2.4. Endothelial cell cytotoxicity

HAECs of passage 9 or 10 were cultured on chamber slides coated with 0.2% gelatin (Nalge Nunc International Corp., Naperville, IL, USA) up to confluence. On the day of the experiment, nanoparticles corresponding to a final iron concentration of 50 μg ml^{-1} were added to cells in triplicate wells with 1 ml of fresh medium. The particles were incubated for 1 h with the cells at 37 °C in an atmosphere containing 5% CO_2. After washing with medium at 37 °C, an equal volume (200 μl each) of culture medium and an ethidium bromide/acridine orange solution was added to the cells. The numbers of dead (stained orange with ethidium bromide) and live (stained green with acridine orange) cells were counted using a ZEISS Axiovert S100 inverted fluorescence microscope (Carl Zeiss Jena GmbH, Jena, Germany). Cells in three different visual fields were counted and the average value ±SD is given. After washing off the particles, cells in the two remaining wells were further cultured in endothelial cell culture medium, and the cytotoxicity was assessed also after 5 and 24 h.

2.5. Light microscopy

HAECs were cultured up to confluence in six-well tissue culture plates coated with 0.2% gelatin using medium 200 and a

low serum growth supplement (LSGS) kit (Cascade Biologics Inc., Portland, OR, USA). Nanoparticles corresponding to a final iron concentration of 50 μg ml^{-1} were added to cells in triplicate wells in 2 ml of fresh medium. The particles were incubated for 1 h with the cells at 37 °C in an atmosphere containing 5% CO_2. The cells were washed once after 1 h using culture medium at 37 °C, and further cultured for another 3, 20 and 24 h in fresh medium. Endothelial cell morphology was assessed in an inverted microscope (Nikon Eclipse TE 300, Nikon Corporation, Tokyo, Japan), at a magnification of 40×. Images were captured using a DXM1200 Nikon digital still camera (Nikon Corporation) and the Nikon act 1 software (Nikon Corporation), and were further processed using Photoshop software (Adobe Systems, San Jose, CA, USA).

2.6. Scanning electron microscopy (SEM)

HAECs were cultured on 8 μm pore size polycarbonate filters (coated with 0.2% gelatin) in tissue culture inserts of 6.5 mm diameter (Transwell, Costar, Cambridge, MA) for at least five days. When the cells had reached confluence, the magnetic nanoparticles were added in fresh medium at a final iron concentration of 50 μg ml^{-1} and incubated with the cells for 1 h. After incubation, the wells were washed once with pre-warmed medium. The cells were fixed by immersion of the wells for 2 h at room temperature in 2% glutaraldehyde in a buffer containing 0.1 M sodium cacodylate, 0.1 M sucrose and 3 mM $CaCl_2$, pH 7.4. After fixation, wells were briefly rinsed in distilled water, then placed in 70% ethanol for 10 min and in 99.5% ethanol for 15 min, all at 4 °C. Wells were then dried in a critical point dryer (CPD010, Balzers, Liechtenstein) with carbon dioxide. After drying, the membranes were cut off, mounted on an aluminium stub and coated with a 15 nm thick platinum layer (Baltec SCD 005, Liechtenstein). The specimen was analysed in a Jeol JSM-820 scanning electroscope at 25 kV.

2.7. Transmission electron microscopy (TEM)

Cells were fixed in 2% glutaraldehyde in 0.1 M sodium cacodylate buffer containing 0.1 M sucrose and 3 mM $CaCl_2$, pH 7.4, at room temperature for 30 min. The cells were scraped off with a wooden stick, transferred to an Eppendorf tube and further fixed overnight in the refrigerator. After fixation, cells were rinsed in 0.15 M sodium cacodylate buffer containing 3 mM $CaCl_2$, pH 7.4, and centrifuged. The pellet was infiltrated with warm (40 °C) 10% gelatin for 15 min, placed in a refrigerator for 10 min and fixed in the same fixative as above overnight. The gelatin block was removed from the tube and the cell pellet was cut by a razor and stored in buffer. The pellets were postfixed in 2% osmium tetroxide in 0.07 M sodium cacodylate buffer containing 1.5 mM $CaCl_2$, pH 7.4, at 4 °C for 2 h, dehydrated in ethanol followed by acetone and embedded in LX-112 (Ladd, VT, USA). Sections were contrasted with uranyl acetate followed by lead citrate and examined in a Tecnai 10 transmission electron microscope (Fei, The Netherlands) at 80 kV.

2.8. Quantification of particle adhesion/phagocytosis by magnetic measurements in the susceptometer

HAECs were cultured up to confluence on six-well tissue culture plates coated with 0.2% gelatin. Magnetic nanoparticles were added in 2 ml of fresh medium to a final iron concentration of 50 μg ml^{-1} and incubated with the cells for 1 h. After the incubation, the supernatants were carefully sucked off and stored in safe-lock Eppendorf tubes. The cells were washed once with 1 ml pre-warmed medium, which was sucked off and pooled with the supernatant from the incubation. The endothelial cells were lysed in 500 μl of lysis buffer (10 mM tris-Cl, pH 7.5, 150 mM NaCl, 1% Triton X-100), which was collected in a separate tube. In order to reduce the viscosity of the lysate, 20 μg of DNase in PBS were added. All samples were prepared in triplicate. Before measuring the sample in the susceptometer, the tubes were flicked vigorously and an aliquot of 60 μl was transferred into a 200 μl, thin-walled PCR tube (Robbins Scientific Corporation, Sunnyvale, CA, USA). Each tube measurement was made three times. A standard curve was prepared by correlating the magnetic susceptibility to the concentration of iron (0–100 μg ml^{-1}) for each particle type. Thus, the smallest detectable concentration of iron in these systems is about 1 μg ml^{-1}.

Measurements on an empty tube, a tube with medium alone, a tube with endothelial cell supernatant without particles and a tube with lysed endothelial cells without particles, as controls, were made. All the data were calculated and analysed using the Microsoft Excel software (Microsoft, Seattle, WA, USA), and the averages of three experiments are given, ±SD.

2.9. Statistical analyses

Results are expressed as mean values, ±SD. The statistical difference between groups was determined by the Mann–Whitney U test. Statistical significance was defined as $p < 0.05$.

3. Results

3.1. Endothelial cell cytotoxicity

The effect of magnetic nanoparticles on endothelial cell viability was assessed in cytotoxicity assays in which confluent monolayers of human aortic endothelial cells were incubated for 1, 5 and 24 h with particles having different coatings. Except for D plain (93%, $p < 0.05$) and D PEG 300 (91%, ns) particles, which induced a slightly suppressed EC viability at 1 h compared to that without particles, none of the tested particles had a deleterious effect on EC viability (table 3).

3.2. Endothelial cell morphology as assessed by light microscopy

The morphology of HAECs following incubation of the cells with D plain, D COOH, D PEG-COOH, D PEG 300 and silica C18 for 1, 3, 20 and 24 h was assessed using inverted phase contrast microscopy at a magnification of 40×. For two of the particles, D COOH and D PEG 300, clearly visible agglomerates were detected both before and after washing away the particles after the 1 h incubation (figures 8(C) and (D),

Table 2. Characteristics of the used nanosized particles.

Particle type	Surface	Mean diameter (nm)[a] (P.I.)[c]	Content of solid (mg ml^{-1})	Fe concentration (mg ml^{-1})[b]	Zeta potential (mV) at pH = 7[d]	Zeta potential zero crossover (pH)[d]
Nanomag®-D	Plain	148 (0.206)	10	6.7	−13.3	5.06
Nanomag®-D	COOH	186 (0.103)	10	5.7	−25.6	4.73
Nanomag®-D	PEG-COOH	241 (0.030)	10	6.7	−17.4	5.00
Nanomag®-D	PEG 300	179 (0.195)	10	5.4	−35.0	3.97
Nanomag®-silica	C18	204 (0.083)	10	7.0	−13.6	3.41

[a] Hydrodynamic diameter (Z_{Ave}): determined by photon correlation spectroscopy (PCS, Zetasizer, Malvern Instruments Ltd, UK).
[b] Determination by use of the Spectroquant® colorimetric iron test (Merck KGaA, Germany).
[c] Polydispersity index.
[d] Detection in 10^{-4} M KCl solution (Zetasizer, Malvern Instruments Ltd, UK).

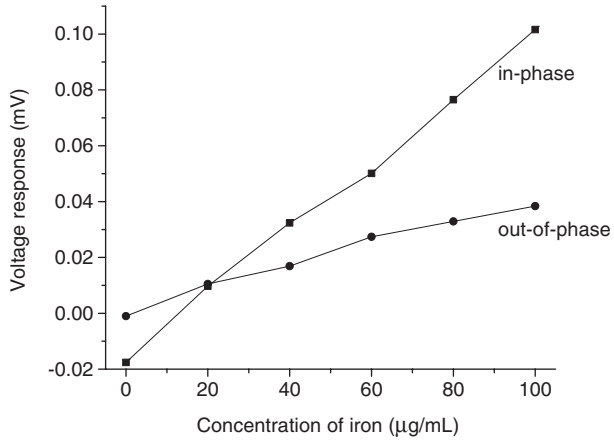

Figure 7. Voltage (susceptibility) versus concentration (expressed as μg ml^{-1} of iron) of D plain suspension in a 60 μl sample at 300 K, 600 A m^{-1} and 2 kHz. This is a typical example of a standard curve relating concentration to susceptibility. Note the negative in-phase susceptibility at low concentrations due to the diamagnetic fluid.

and (G) and (H)). ECs incubated with agglomerated particles still had visible agglomerates for up to 23 h post-washing (not shown). Other particle types were hardly visible even before washing off the particles at the end of the incubation time (figures 8(A), (E) and (I)). Incubation of HAECs with the different particles had no effect on EC morphology as detected by inverted phase contrast microscopy.

3.3. Quantification of endothelial cell–particle adhesion/phagocytosis using a desktop susceptometer

We used the desktop susceptometer to quantify the amount of magnetic material in the culture medium supernatants and lysed cells recovered after incubation with the various particles (figure 9). The amount of recovered magnetic material in the supernatant or the fraction associated with the cells varied between the particle types (figure 9). The D plain, D PEG-COOH and silica C18 interacted to a very low degree with the endothelial cells, with most of the iron recovered in the supernatant (figure 9). In bright contrast, a substantial fraction of the D PEG 300 (26%) and D COOH (58%) particles remained adhered to, or phagocytosed by, the ECs following washing. The increased cell interaction seen with these particle types was in line with visible light microscopy, since remains of these particles could be seen with the cells following washing (figure 8).

Table 3. Human aortic endothelial cell viability following incubation with nanoparticles with different surface characteristics at a final iron concentration of 50 μg ml^{-1} (note: ND stands for not determined).

	Incubation time/% live cells		
Particles	1 h	5 h	24 h
No of particles	98	ND	ND
Plain	93	97	99
COOH	99	98	98
PEG-COOH	97	98	96
PEG 300	91	98	98
Silica C18	97	99	99

3.4. Endothelial cell morphology as assessed by scanning electron microscopy

Particle adhesion to the EC surface varied and depended on the particle coating (figure 10). Confirming the magnetic measurements, D COOH coated particles adhered to a large extent and appeared as agglomerates on the cell surface as revealed by SEM (figures 10(b) and (c)). Little adhesion after washing was seen for D plain (figure 10(a)), D PEG-COOH (figure 10(d)), D PEG 300 (figure 10(e)) and silica C18 (figure 10(f)) particles. The inadequacy of using SEM observations for quantitative estimations is illustrated in figure 10(c), in that some areas of the cell monolayer were devoid of particles (in this case D COOH), whereas other areas had a high number of particles attached.

3.5. Endothelial cell morphology as assessed by transmission electron microscopy

Particle phagocytosis was revealed by TEM (figure 11). In convincing agreement with the magnetic measurements, with substantial fractions of particles coated with D COOH (about 58%) and D PEG 300 (about 26%) being associated with the endothelial cells (figure 9), these particles were phagocytosed to a large extent (figures 11(b) and (d)). This is revealed by the rich accumulation of electron-dense material in large endosomes. A very low degree of phagocytosis was seen for D plain (figure 11(a)), D PEG-COOH (figure 11(c)) and silica C18 (figure 11(e)) particles.

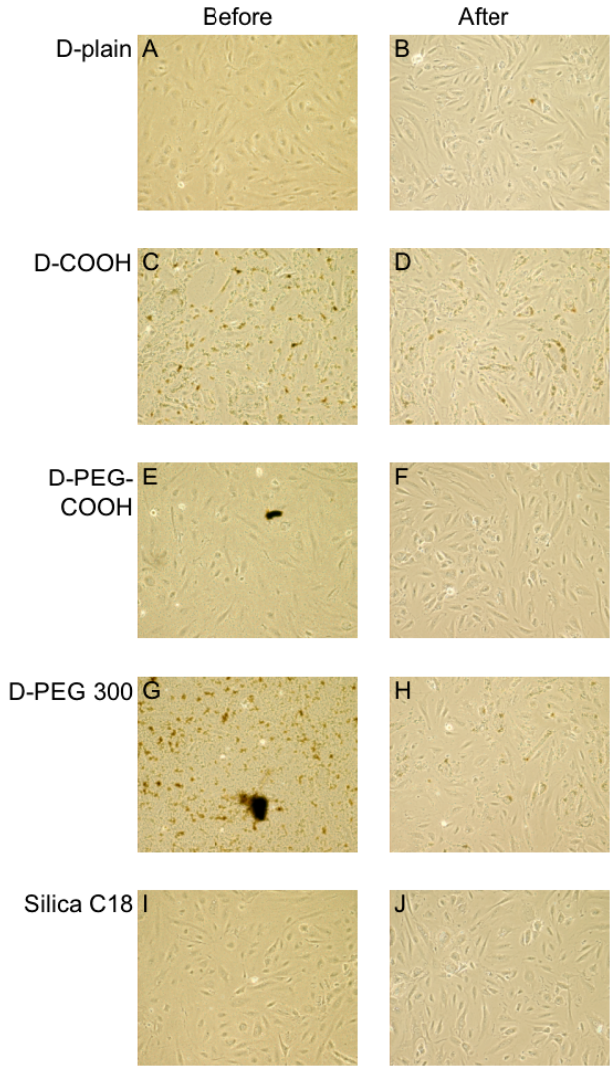

Figure 8. Inverted phase contrast microscopy of human aortic endothelial cells incubated for 1 h at 37 °C with D plain ((a) and (b)), D COOH ((c) and (d)), D PEG-COOH ((e) and (f)), D PEG 300 ((g) and (h)) and silica C18 ((i) and (j)) particles. The concentration of particles is 50 μg ml^{-1} of iron. The cells were observed at a magnification of 40× and pictures were taken before (left) and after (right) washing the cells once with pre-warmed culture medium.

(This figure is in colour only in the electronic version)

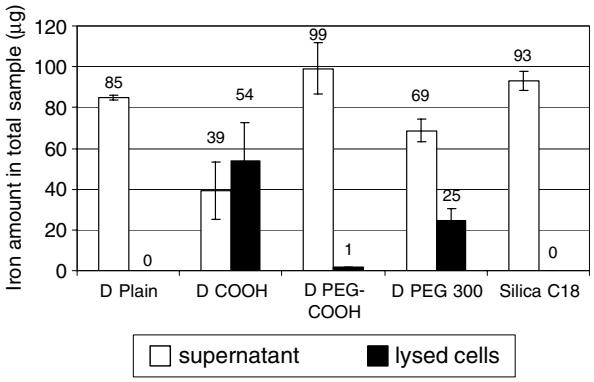

Figure 9. Quantification of endothelial cell–particle interactions using the desktop susceptometer. Each sample was incubated with particles corresponding to 100 μg of iron. Following a 1 h incubation with the particles, an aliquot of 60 μl of the supernatant containing particles not interacting with the cells, and 60 μl of a cell lysate were measured. Standard curves correlating magnetic susceptibility with iron concentration were obtained for each particle type. The measurement results are presented as the amount of iron in the total sample, so the sum of the supernatant and lysis responses should nominally equal 100 μg. The average of three experiments is given, ±SD.

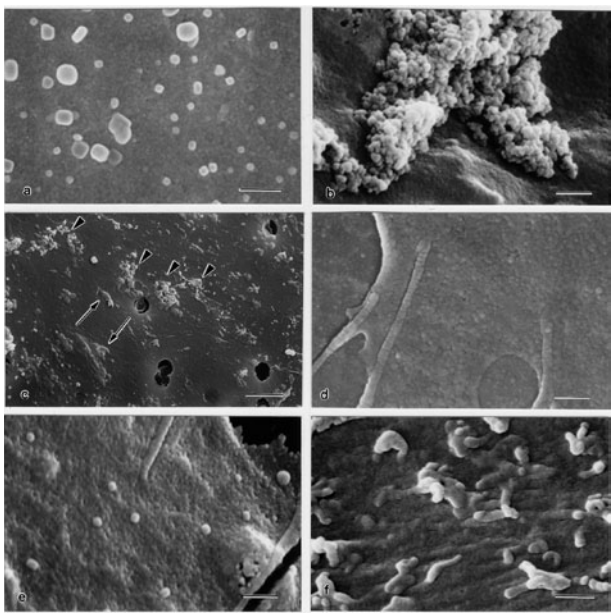

Figure 10. Scanning electron micrographs of human aortic endothelial cells incubated with D plain (a), D COOH ((b) and (c)), D PEG-COOH (d), D PEG 300 (e) and silica C18 (f) particles for 1 h and then washed. The bar length is 1 μm. Arrow-heads point at agglomerated particles, and arrows at an uneven cell layer.

4. Discussion

The ultimate goal of drug delivery is to specifically target a diseased cell population in the body using tailored pharmaceutical compositions. In order to develop such drug delivery systems based on surface modified nanoparticles, it is imperative to assess in an accurate, quick and simple way the level of interaction between the particle and the target cell type using various adhesion assays *in vitro*. For this purpose, we have developed a desktop magnetic susceptometer, which allowed us to rapidly and in a simple fashion quantify the interaction of magnetic nanosized particles with endothelial cells.

Traditionally, the uptake of magnetic particles by cells has been qualitatively demonstrated using electron microscopy or immunofluorescence methods [16–18]. Quantification using these methods is difficult though. Nuclear magnetic resonance relaxometry has been used to estimate magnetic particle concentration in cell samples or organs *ex vivo* [19]. However, this method suffers from the relaxivity seeming to be strongly dependent on whether the magnetic particles are internalized and concentrated in intracellular organelles [20]. Conventional magnetometry using e.g. a superconducting quantum interference device (SQUID) or vibrating sample magnetometer (VSM) could be used, but is time-consuming, costly and needs considerable user experience and is therefore not very tractable. Recently, Wilhelm *et al* [21] reported

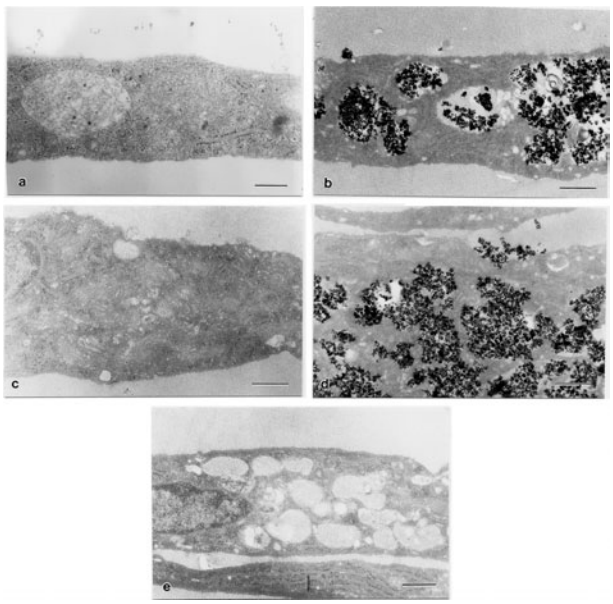

Figure 11. Transmission electron micrographs of human aortic endothelial cells incubated with D plain (a), D COOH (b), D PEG-COOH (c), D PEG 300 (d) and silica C18 (e) particles for 1 h and then washed. The bar length is 1 μm. Note the marked accumulation of clusters of dense (presumably iron rich) material in items (b) and (d).

on the use of magnetophoresis and ferromagnetic resonance (FMR) to quantify the uptake of magnetic nanoparticles in phagocytic and non-phagocytic cells. In the first method, magnetophoresis, the velocity of an individual cell movement in a magnetic gradient is measured and in the second (FMR) the combined electronic spin of a bulk sample is quantified [21]. A quantitative agreement was found between the methods with regard to particle phagocytosis by macrophages and other cell types. Due to sedimentation effects the smallest resolvable uptake using magnetophoresis was stated as 0.1 pg of particulate iron per cell [21]. Although highly interesting as a means of studying the particle uptake of individual cells, this method might not be appropriate for assays involving many samples, especially so since the method requires a sufficiently low concentration of particles to avoid particle interactions. In the FMR method, the smallest detectable quantity is stated as an amount of about 2.5 ng of iron [21]. In the sample volume of 5 μl, this equals an iron concentration of 0.5 μg ml^{-1}, which is somewhat lower than our corresponding value of 1 μg ml^{-1}. Although these two values happen to be rather similar, it must be kept in mind that the particles are not the same and that the measured magnetic properties are very dissimilar. More important issues are sample preparation, speed and complexity of the apparatus. Concerning a practical application for concentration determination, the susceptibility method might be preferred, since it requires no further sample relocation into minute 5 μl pipettes as FMR does, and needs little more than a few seconds for a measurement.

An accumulation of white blood cells in a particular tissue/organ is called an inflammatory reaction. Many diseases which afflict a large portion of the population are characterized by inflammation. The inflammatory reaction is important for the healing process, for instance during wound healing, but may, if uncontrolled, also be the main cause of the disease itself, for instance in the case of autoimmune diseases, reperfusion injury and graft rejection. The most important regulator of inflammation is the endothelium [22]. With some exceptions, white blood cells interact to a very low degree with endothelium at rest, i.e. they stay in the blood stream. However, following for instance a microbial infection, the endothelium is activated and, as a result of this activation, it expresses cell adhesion molecules and chemoattractant molecules which facilitate the extravasation of white blood cells [23]. We have embarked on a project aiming at targeting magnetic nanoparticles to activated endothelium. An important stepping-stone in this effort is to develop methods and equipment, i.e. the desktop susceptometer, by means of which we can rapidly quantify specific particle adhesion to activated endothelium under static and dynamic conditions *in vitro*.

In order to develop nanoparticles which can be targeted to activated endothelial cells following intravenous administration [24, 25], such particles must have characteristics making them long-circulating, i.e. they should not be phagocytosed by the mononuclear phagocyte system nor should they, due to their size, be trapped in the spleen [26]. The propensity to phagocytosis and short serum half-lives of nanoparticles in serum is related to the surface characteristics such that a steric barrier of a hydrophilic polymer reduces phagocytosis [26, 27]. Examples of such polymers are poly(ethylene oxide), poly(ethylene glycol) and the polysaccharides, dextran and heparin [28, 29]. We used particles of different surface characteristics (hydrophilicity/hydrophobicity and surface charge), but without specific targeting molecules, in order to investigate their interaction with resting endothelial cells. The PEG 300 particles appeared slightly cytotoxic to the endothelial cells at 1 h as compared to the other particles (table 3). This may be explained by the high degree of phagocytosis of this particle by ECs (figure 11(d)). However, the D COOH particles with the D COOH surface interacted even more with ECs (figure 9) and were also phagocytosed to a large extent (figure 11(b)), but not cytotoxic to the cells (table 3). It is not clear to us why the PEG 300 particles and not the others were slightly cytotoxic. The fact that the D COOH and PEG 300 particles interacted to a much higher degree with the endothelial cells cannot be easily explained in terms of hydrophilicity. However, both of these particles appeared agglomerated on the surface of the endothelium (figures 8(C), (D), (G) and (H), and 10(b) and (c)) and had lower zeta potentials at pH 7 than the other particles (table 3). Previous studies have shown that a particle zeta potential close to zero reduced phagocytosis in comparison with the case for charged particles, particularly those of positive surface charge [30]. Thus, the lower zeta potential of D COOH and PEG 300 particles may increase EC adhesion/phagocytosis by itself, or may make the particles susceptible to agglomeration in the culture medium used. This agglomeration may stimulate adhesion and phagocytosis by engagement and cross-linking of a larger population of surface receptors. It is well known that phagocytosis occurs mainly with larger particles (>0.5 μm) [31], and particle agglomeration may thus be the reason for the high degree of phagocytosis seen with the D COOH and D PEG 300 particles. Even though the behaviour of the particles with cells *in vitro* can be studied

in some detail, the fate of a particular particle *in vivo* is hard to predict since it is affected by factors (e.g. protein opsonization) that cannot be easily mimicked in the *in vitro* cell culture models. Thus, particle biodistribution profiles following intravenous administration need to be established in small animal models.

In conclusion, we have described the construction of a novel desktop susceptometer that can be used to quantify the interaction of magnetic particles with cells in a simple manner, which will allow us to optimize *in vitro* the interaction of surface-tailored, magnetic nanoparticles with the desired target cell type.

Acknowledgments

This work was supported by the European Community under the 'Competitive and Sustainable Growth' programme (GRD1-2000-25126) and the Swedish Research Council, No K2002-06X-13031-01A. JH holds a position within the programme 'Glycoconjugates in Biological Systems' financed by the Swedish Foundation for Strategic Research. We gratefully appreciate having full access to the facilities within Prof K V Rao's group at the MSE department and having benefitted from skilled SQUID measurements performed by Ms Amita Gupta. We are also grateful to Mrs Eva Ström for her contribution of an artistic interpretation of the sample insertion procedure shown in figure 3.

References

[1] Safarik I and Safarikova M 1999 Use of magnetic techniques for the isolation of cells *J. Chromatogr.* B **722** 33
[2] Thiel A, Scheffold A and Radbruch A 1998 Immunomagnetic cell sorting—pushing the limits *Immunotechnology* **4** 89
[3] Luxembourg A T, Borrow P, Teyton L, Brunmark A B, Peterson P A and Jackson M R 1998 Biomagnetic isolation of antigen-specific $CD8^+$ T cells usable in immunotherapy *Nat. Biotechnol.* **16** 281
[4] Olsvik O *et al* 1994 Magnetic separation techniques in diagnostic microbiology *Clin. Microbiol. Rev.* **7** 43
[5] Uhlen M 1989 Magnetic separation of DNA *Nature* **340** 733
[6] Sumitran-Karuppan S 1999 The clinical importance of choosing the right assay for detection of HLA-specific donor-reactive antibodies *Transplantation* **68** 502
[7] LaVan D A, Lynn D M and Langer R 2002 Moving smaller in drug discovery and delivery *Nat. Rev. Drug Disc.* **1** 77
[8] Weissleder R 2002 Scaling down imaging: molecular mapping of cancer in mice *Nat. Rev. Cancer* **2** 1
[9] Lewin M *et al* 2000 Tat peptide-derivatized magnetic nanoparticles allow *in vivo* tracking and recovery of progenitor cells *Nat. Biotechnol.* **18** 410
[10] Schutt W *et al* 1997 Applications of magnetic targeting in diagnosis and therapy—possibilities and limitations: a mini-review *Hybridoma* **16** 109
[11] Lübbe A S *et al* 1996 Clinical experiences with magnetic drug targeting: a phase I study with 4′-epidoxorubicin in 14 patients with advanced solid tumors *Cancer Res.* **56** 4686
[12] Schutt W *et al* 1999 Biocompatible magnetic polymer carriers for *in vivo* radionuclide delivery *Artif. Organs* **23** 98
[13] Goldfarb R B, Lelenthal M and Thompson C A 1992 *Alternating Field Susceptometry and Magnetic Susceptibility of Superconductors* (New York: Plenum)
[14] Hartshorn L 1925 The properties of mutual inductance standards at telephonic frequencies *J. Sci. Instrum.* **2** 145
[15] Grüttner C and Teller J 1999 New types of silica-fortified magnetic nanoparticles as tools for molecular biology applications *J. Magn. Magn. Mater.* **194** 8
[16] Schulze E, Ferrucci J J, Poss K, Lapointe L, Bogdanova A and Weissleder R 1995 Cellular uptake and trafficking of a prototypical magnetic iron oxide label *in vitro Invest. Radiol.* **30** 604
[17] Moore A, Weissleder R and Bogdanov A 1997 Uptake of dextran-coated monocrystalline iron oxides in tumor cells and macrophages *J. Magn. Reson. Imaging* **7** 1140
[18] Dodd S J, Williams M, Suhan J P, Williams D S, Koretsky A P and Ho C 1999 Detection of single mammalian cells by high-resolution magnetic resonance imaging *Biophys. J.* **76** 103
[19] Rety F *et al* 2000 MR lymphography using iron oxide nanoparticles in rats: pharmocokinetics in the lymphatic system after intravenous injection *J. Magn. Reson. Imaging* **12** 734
[20] Oswald P, Clement O, Chambon C, Schouman-Claeys E and Frifa G 1997 Liver positive enhancement after injection of superparamagnetic nanoparticles: respective role of circulating and uptaken particles *Magn. Reson. Imaging* **15** 1025
[21] Wilhelm C, Gazeau F and Bacri J-C 2002 Magnetophoresis and ferromagnetic resonance of magnetically labeled cells *Eur. Biophys. J.* **31** 118
[22] Koning G A, Schiffelers R M and Storm G 2002 Endothelial cells at inflammatory sites as target for therapeutic intervention *Endothelium* **9** 161
[23] Springer T A 1994 Traffic signals for lymphocyte recirculation and leukocyte emigration: the multistep paradigm *Cell* **76** 301
[24] Spragg D D *et al* 1997 Immunotargeting of liposomes to activated vascular endothelial cells: a strategy for site-selective delivery in the cardiovascular system *Proc. Natl Acad. Sci. USA* **94** 8795
[25] Blackwell J E, Dagia N M, Dickerson B, Berg E L and Goetz D J 2001 Ligand coated nanosphere adhesion to E- and P-selectin under static and flow conditions *Ann. Biomed. Eng.* **29** 523
[26] Moghimi S M, Hunter A C and Murray J C 2001 Long-circulating and target-specific nanoparticles: theory to practice *Pharmacol. Rev.* **53** 283
[27] Davis S S 1997 Biomedical applications of nanotechnology—implications for drug targeting and gene therapy *Trends Biotechnol.* **15** 217
[28] Jaulin N, Appel M, Passirani C, Barrat G and Labarre D 2000 Reduction of the uptake by a macrophagic cell line of nanoparticles bearing heparin or dextran covalently bound to poly(methyl methacrylate) *J. Drug Target.* **8** 165
[29] Moghimi S M and Hunter A C 2001 Capture of stealth nanoparticles by the body's defences *Crit. Rev. Ther. Drug Carrier Syst.* **18** 527
[30] Roser M, Fischer D and Kissel T 1998 Surface-modified biodegradable albumin nano- and microspheres. II: effect of surface charges on *in vitro* phagocytosis and biodistribution in rats *Eur. J. Pharm. Biopharm.* **46** 255
[31] Aderem A and Underhill D M 1999 Mechanisms of phagocytosis in macrophages *Annu. Rev. Immunol.* **17** 593